Chapter 6

The atmospheric boundary layer over melting glaciers

J. Oerlemans

Institute for Marine and Atmospheric Research, at Utrecht University, Utrecht, the Netherlands.

Abstract

Results from a number of glacio-meteorological experiments carried out over melting glaciers are summarized. It is shown that in summer the microclimate of a glacier tongue is dominated by katabatic flow, initiated by the downward sensible heat flux. Characteristic obstacle height is an appreciable fraction (typically 0.1 to 0.5) of the height at which the wind maximum occurs, implying a serious zero-reference problem for profile analysis. Using a bulk method with roughness length estimated by a micro-topographic method appears to perform better. Analysis of the momentum and heat budgets shows that, in a first-order approximation, the dynamics of this flow can be described well by the classical Prandtl model for slope winds. The Prandtl model is extended by introducing a flow-dependent eddy viscosity. The eddy viscosity is set proportional to the maximum wind velocity (velocity scale) and the height at which the wind maximum occurs (length scale). An analytic solution can then be obtained which provides a useful description of the katabatic flow and the associated exchange of heat with the glacier surface.

1 Introduction

Glaciers and ice sheets affect human activities in several ways. On a regional scale, glaciers supply melt water for hydropower reservoirs and for irrigation systems. Sudden unexpected events, like ice avalanches and outbursts of glacier-dammed lakes have caused disasters. Even the more common fluctuations in the size of a glacier may threaten roads, constructions and property. It is also believed that glaciers and ice sheets have contributed substantially to sea-level fluctuations on the century time scale, and will do so in the near

future (Warrick, 1996).

Valley glaciers register climate fluctuations. Melting is a process that is very sensitive to air temperature variations. Because in the case of a melting glacier the surface temperature is fixed, a higher air temperature immediately leads to a larger downward sensible heat flux and an increase in the longwave radiation balance. A direct manifestation of this large sensitivity is the impressive change that valley glaciers underwent in the last century (Oerlemans, 1994). So, from the point of view of the climatologist, historical records of glacier length contain valuable information on climate change.

Ice sheets register climate fluctuations on a larger time scale. It is not variations in the size of ice sheets which provide information, but the fact that the central parts of the big ice sheets are relatively stable and therefore contain old ice at a great depth. The physical properties of this ice and the air bubbles enclosed in it contain a wealth of information on earlier climate and atmospheric composition. So far, ice with an age of up to 300 000 years has been analysed successfully.

In many applications, time-dependent simulation of glacier geometry with numerical models has become an important tool. Such applications range from simulating the history of the Greenland ice sheet during the last 200 000 years (to help with the interpretation of results from ice cores) to predicting how a particular glacier threatening a dam will behave in the next 50 years. Crucial in such calculations is the formulation of the mass balance. Relating the surface mass balance to general climatological conditions requires a good understanding of the processes in the boundary layer that control the exchange of heat and moisture.

For a long time it has been noted that on fair summer days shallow downslope winds develop over melting glaciers (Tollner, 1931; Hoinkes, 1954). In fact, melting glaciers form a unique laboratory for the study of katabatic winds, since the surface temperature remains at the melting point for long periods of time (sometimes for several months), providing a simple lower boundary condition for temperature and vapour pressure. The katabatic flow down glaciers has been termed glacier wind. A number of meteorological investigations on melting glaciers surfaces have taught us a great deal about the significant micrometeorological processes that determine melt (Ambach, 1963; Björnsson, 1972; Wendler and Weller, 1974; Martin, 1975; Munro and Davies, 1978; Hogg et al., 1982; Munro, 1989; Ohata et al., 1989; Ishikawa et al., 1992). Nevertheless, most of these studies were restricted to a single location and/or were of short duration.

Recently more extensive meteorological experiments have been performed in which five or more stations were operated simultaneously (Oerlemans and Vugts, 1993; Greuell et al., 1994; TEMBA, 1997). In this paper selected results from these experiments are discussed. The emphasis will be on the phenomenology and modelling of the glacier wind and the related exchange of energy between glacier surface and atmosphere.

2 Field experiments and data sources

Before we present data, some comments are made on the difficulties of operating weather stations on glaciers. Access is difficult, notably in the ablation zone. In late spring / early summer the snow pack is wet and when drainage is poor swamp-like conditions exist. Later in the melt season the ice surface becomes rough and the only means of transport is by helicopter. The shape of the surface is constantly changing. A typical melt rate is 5 m of ice in one summer. Therefore instruments mounted on structures drilled into the ice protrude further and further from the surface. To solve this problem, at the Institute for Marine and Atmospheric Research (Utrecht University) a construction has been developed that stands freely on the ice and sinks with the melting surface. Another difficulty is power supply. Ventilators for temperature sensors should have a minimum dimension and it is impossible to ventilate radiation sensors unless generators are used. If stations are to operate unattended for a week or so they must be designed with great care.

Table 1. A listing of glacio-meteorological experiments from which the data used in this article originate.

Location	period	equipment	participants
Central West Greenland 0 - 1000 m L $\sim$ 100 km	summer 1991	7 stations RASS-SODAR thethered balloon eddy correlation meas. 31 m profile mast	IMAU Free University Amsterdam
Pasterze Austria 2000 - 3400 m L $\sim$ 10 km	summer 1994	7 stations thethered balloon eddy correlation meas. 13 m profile mast	IMAU Free University Amsterdam
Vatnajökull Iceland 0 - 1600 m L $\sim$ 50 km	summer 1996	12 stations radiosonde thethered balloon eddy correlation meas. measurements	IMAU Free University Amsterdam University of Iceland University of Innsbruck

The logistics are complicated, but the experiments rewarding. Table 1 lists three summer experiments in which valuable data sets on the structure of katabatic flows over melting glacier surfaces were obtained. As noted earlier, the most significant difference between these studies and earlier observational studies on melting glaciers is that many stations were operated at the same time to obtain insight into altitudinal gradients. The melt zones studied in the summer experiments first of all differ in size (characteristic scale L of melt area in downslope direction) and in their climatic setting. For the transect on the Greenland ice sheet there is lateral symmetry to a large extent. The climatic conditions are dry (annual precipitation of the order of 0.3 m), relatively sunny and with a large annual temperature range (about 28 K). The melt season is short. The situation on the Pasterze is very different: the flow is channelled by the valley walls. The melt season is much longer and a typical figure for the annual amount of melt is 5 m. The climatic conditions on Vatnajökull, which is the largest ice cap in Iceland (and Europe) and covers an area of 8000 km^2, are very maritime: high precipitation and a relatively small seasonal cycle in temperature (Björnsson, 1988). The mass turnover is very large: high accumulation of snow in the upper parts of the ice cap is compensated by large melt rates in the lower parts (up to 10 m of ice per year).

3 Occurrence of the glacier wind

The first question to consider is how often a well-defined katabatic layer occurs. One way to find out is to look at the persistence of the glacier wind at various sites. This persistence can be defined in several ways. Here we look at histograms of wind direction for a few selected sites (Figure 1). From the Pasterze experiment (PASTEX) results from two stations are shown. Site 5 is close to the highest point and exposed, site 3 is in the middle of the well-defined glacier tongue. The character of the histograms is totally different: at site 5 there is no dominating wind direction. In contrast, at site 3 the flow is almost always down the glacier.

Unfortunately, in the Greenland experiment no station could be operated on the ice divide. The graphs shown here are for stations close to the ice edge (site 4) and about 40 km from the ice edge (site 6, which is still about 200 km from the ice divide). For site 6 on Greenland the histogram peaks at a direction about 30 degrees away to the right of the fall line. This points to the importance of the Coriolis acceleration in the momentum budget. Closer to the ice edge, at Greenland 4, the deflection is smaller. This is understandable, as here the strength of the forcing increases due to a larger surface slope and the thermal contrast between tundra and ice sheet (creating a pressure gradient on the mesoscale). For Vatnajökull there is a striking difference between the wind regime on the plateau and on an outlet glacier (Breidamerkurjökull). The

station R3 is in the western part of the plateau and the wind measured there is probably closely correlated with the synoptic-scale flow. In the period considered a preference for southerly and northwesterly winds can be observed. In contrast, on the glacier tongue the flow is always downslope. This is remarkable if one realizes that this glacier tongue is very wide (~ 20 km) and exposed to weather systems coming across the Atlantic.

For all regions considered here, the large-scale flow pattern is highly variable. Nevertheless, all weather stations in the melt zones show that downslope

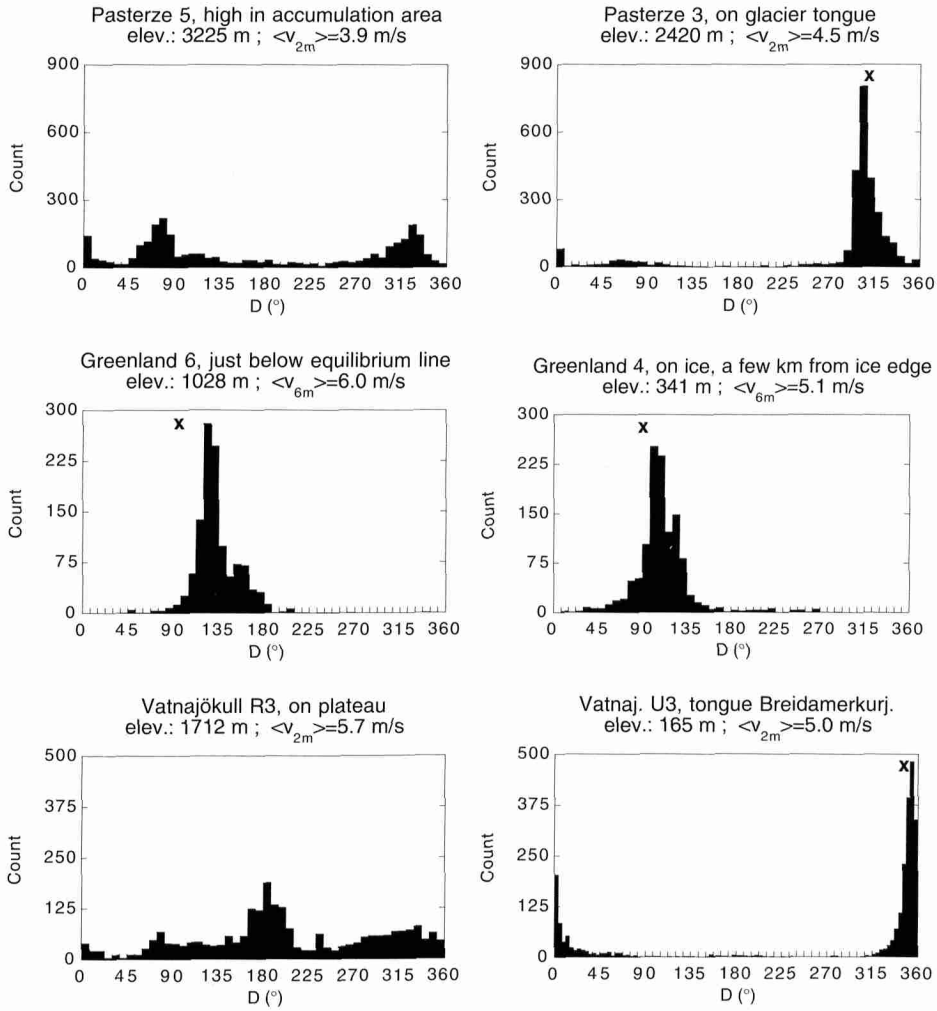

Fig. 1. Histograms of wind direction D for some selected sites on the glaciers studied. The fall line of the local topography is indicated by x. For the Greenland stations hourly mean values of wind direction are used, for the other stations half-hourly mean values. Mean wind speed is denoted by <v>. Note that for the Greenland stations values of <v> refer to a measuring height of 6 m, for the other stations to 2 m.

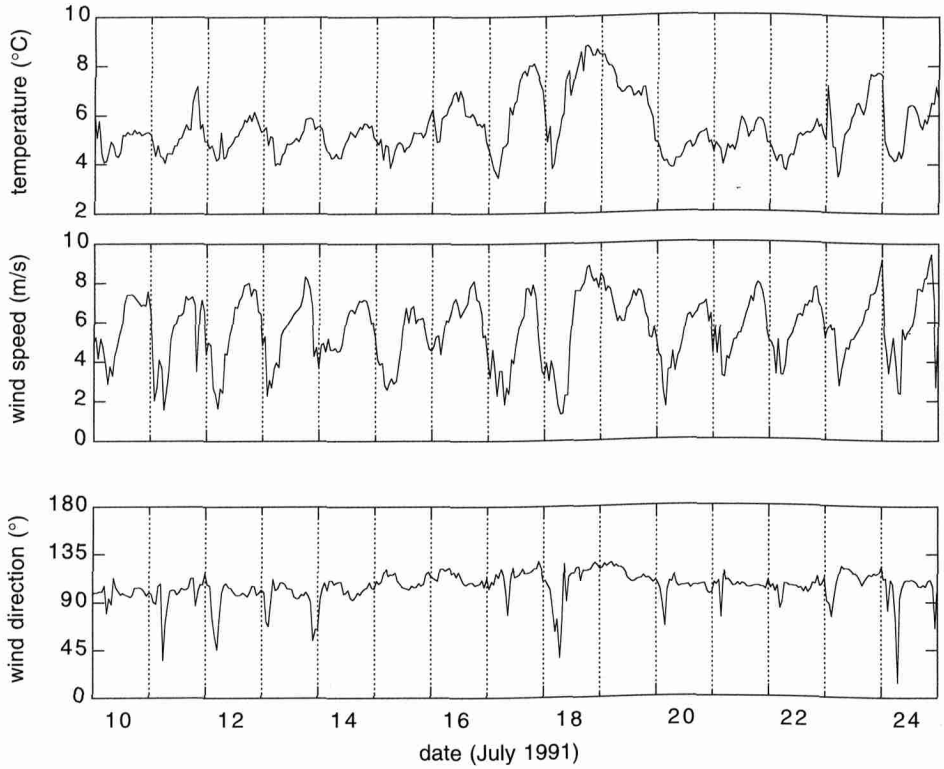

Fig. 2. Daily cycle in the glacier wind as observed on the edge of the Greenland ice sheet. Data shown are for a 16-day fair weather period in the summer of 1991. The graphs display hourly mean values of air temperature, wind speed and wind direction at 6 m. From Oerlemans and Vugts (1993).

flow is definitely the dominating one. Undoubtedly, this flow is of katabatic origin. Although the surface slope is generally small (1 to 5°) the rate at which the air is cooled is fast enough to produce a strong katabatic force. During periods of fair weather, great regularity in the daily rhythm of the glacier wind can be observed. An example from the Greenland ice sheet is shown in Figure 2. First of all it can be seen that air temperature is always well above freezing point. Wind speed reaches maximum values in late afternoon, in phase with air temperature. Typically, through the day the wind speed ranges from 3 to 7 m/s. The wind direction is constant. Only during very calm hours just after midnight does the wind sometimes back from east-southeast to northeast for short periods of time.

The close relation between the air temperature and the strength of the katabatic flow turns out to be a general feature. This suggests that to first order the momentum balance is between buoyancy force (proportional to temperature deficit and surface slope) and friction. A characteristic temperature

deficit in the lower melt zone of the Greenland ice sheet is 5 K [1]. It is easily calculated that for a surface slope of a few degrees the associated katabatic acceleration is typically 0.01 m s^{-2}. For the wind speeds measured this implies that the Coriolis acceleration can only be of secondary importance.

In the Greenland experiment the highest station was at 1510 m a.s.l. Here melt is limited and the daily cycle in air temperature is larger because on sunny days an unstable layer develops just above the snow surface. Inspection of the daily cycle for all stations on the ice sheet (at 341, 519, 1028 and 1510 m a.s.l.) revealed that the katabatic regime changes. In the lower ablation zone the katabatic force is caused by the downward flux of sensible heat. Higher up, radiative cooling at the surface is more important. Consequently, in the lower ablation zone the strength of the katabatic flow reaches its maximum in late afternoon, higher up this occurs late at night (Oerlemans and Vugts, 1993).

4 Vertical structure of the glacier wind - observations

It is not easy to probe the vertical structure of the katabatic flow over a melting glacier surface. Notably in the lower parts of ablation zones, melt rates are so high that it is hard to construct a stable platform for larger devices. During GIMEX-91 (see Table 1), a RASS-SODAR system was operated by the Free University, Amsterdam, at a site close to the equilibrium line (at about 1500 m a.s.l.). Here the melt is restricted and the system could be installed on the surface in a satisfactory way. It is obvious that the strong thermal stratification of the flow and the limited availability of power prevents deep probing of the boundary layer. The data obtained reveal well-developed katabatic flow most of the time, with the wind maximum at a height of typically 30 m. However, there were also a number of days without a well-defined katabatic layer.

Sounding of the katabatic flow by regular radiosondes is not possible, because the speed of ascent is too large. Neither the required resolution, nor a reasonable accuracy of measurement can be obtained. Instead, in the experiments listed in Table 1 use has been made of a tethered zeppelin (11 m^3 helium), carrying an aspirated temperature/humidity sensor as well as sensors for air pressure, and wind speed and direction. This system is able to reach an altitude of typically 1000 m.

During GIMEX-91, the system was operated just in front of the ice edge. Within 51 days 220 ascents were made. In the Pasterze experiment the balloon system was installed on the ice. Here about 200 ascents were made. As the system is rather sensitive to weather conditions (surface wind speed should not exceed 10 m/s and it should not rain) its use was less successful

[1] The temperature deficit is the difference between the temperature of the surface and the air just above the katabatic layer

on Vatnajökull. Nevertheless, about 200 ascents were made just in front of Breidamerkurjökull, and later on the glacier itself.

Altogether, the zeppelin soundings have produced a large data set on the vertical structure of the glacier wind. A few extracts from this material are presented. Figure 3 shows data from the tethered balloon which was operated just in front of the ice edge in Greenland. Each sounding took about 1 hour: 30 minutes to go up, the remaining time to come down. The various quantities were sampled every 10 seconds. All data points were used in the graphs, to give an impression of variability as well as the difference between the up- and down-going soundings. Obviously, when quantities change significantly within an hour, this will be reflected in the graphs. Note, for instance, that the down-going branch for temperature at 06:35 (local time) indicates a 2 K temperature rise in the lower 200 m. The graphs for 06:35 show a structure typical for fair weather conditions: a stable stratification and weak winds throughout the lowest kilometre of the troposphere. Heating at the surface has started. Then a convective mixed layer develops over the tundra and is advected towards the ice sheet.

In the graphs for 12:40 it can be seen clearly that a katabatic wind shoots under the convective layer. The highest wind speed is now found close to the surface, and the wind direction exhibits a marked change (from easterly to westerly) at a height of about 250 m. Note the ragged appearance of the temperature curves, indicative of well-developed convectively-driven turbulence. The surface inversion reaches a value of 3 to 4 K. The profile for 18:35 shows how the mixed layer calms down, but has not yet cooled. In the 12:40 picture, the level at which the wind turns from east to west is much higher than the top of the cold layer (which is at a height of only a few tens of metres). This suggests the existence of a relatively stable layer a few hundreds of metres deep, representing the large-scale katabatic regime. This example as well as soundings from other days show that a return flow at higher levels, by which warm air is advected from the tundra onto the ice sheet, is an important feature of the local atmospheric circulation.

We return to the measurements on the valley glaciers. Detailed observations in the lower 14 metres of the glacier wind were carried out during PASTEX by the Free University, Amsterdam. Sensors were operated at nominal heights of 0.25, 0.5, 1, 2, 4, 6, 8 and 13 m. The mast was located on the glacier, about 500 m from the terminus. At this site the slope of the glacier surface is only about 5 degrees. In most cases where glacier wind occurred the height of the wind maximum was between 2 and 8 m. Results for a typical fair weather day are shown in Figure 4. There is a great regularity in the observed profiles. The height of the wind maximum is at 4 or 6 m. During the day air temperature goes up only a few degrees, and a slight increase in the wind speeds can then be seen. As is obvious from Figure 4, at greater heights the daily cycle is more prominent.

Van den Broeke (1996) made an extensive analysis of the balloon soundings on Greenland and the Pasterze and documented the observed daily cycle

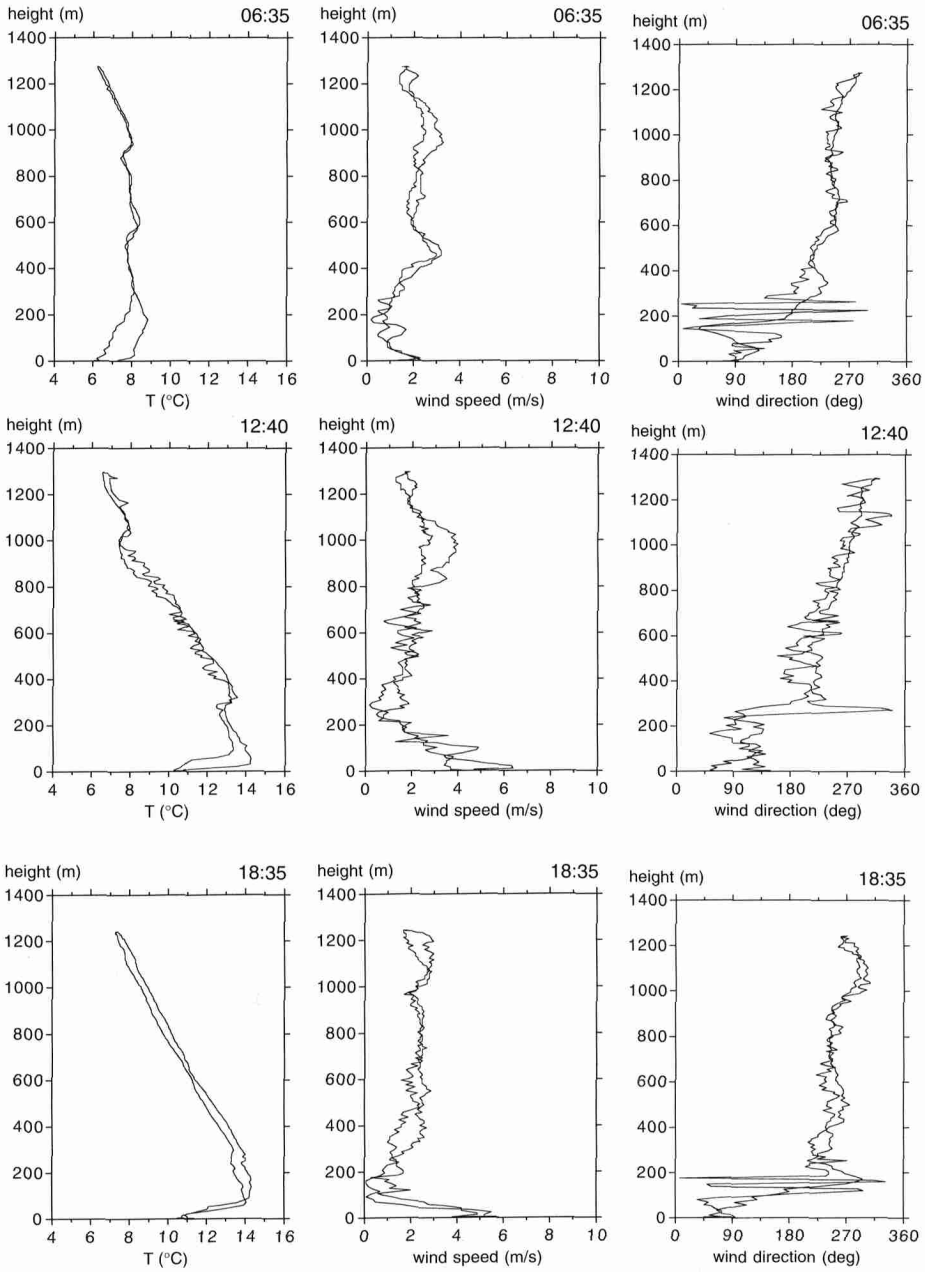

Fig. 3. Temperature and wind profiles obtained at the edge of the Greenland ice sheet on 14 July 1991 with a balloon. In each graph the up- and downgoing branche is shown. From Oerlemans and Vugts (1993).

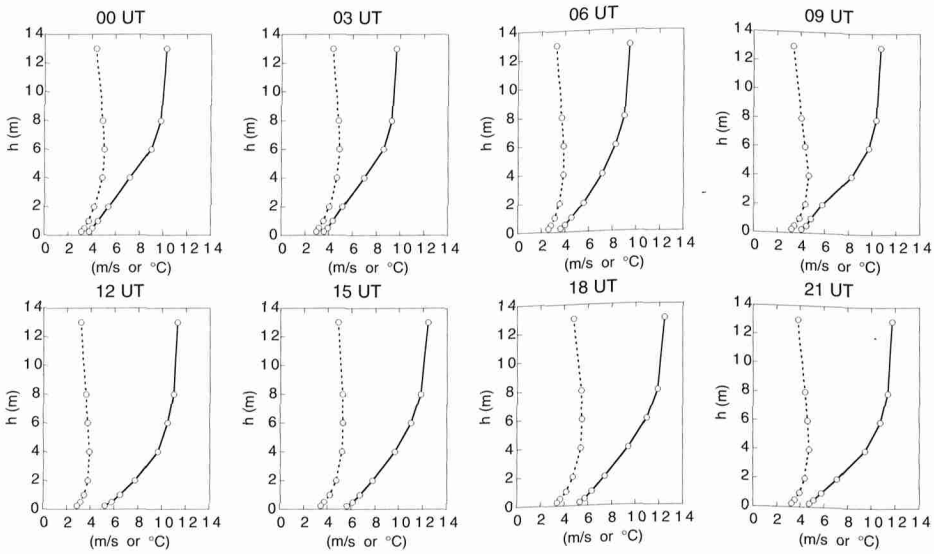

Fig. 4. Measured profiles of temperature (solid) and wind speed (dashed) on a warm summer day (Julian day 210, 1994). Each data point shown represents a 30 min average. Data kindly provided by P. Smeets (Free University, Amsterdam).

in fair weather with weak synoptic-scale forcing. Time-height cross sections for downslope wind component and potential temperature provide inside in the vertical structure of the flow. Figure 5 shows the result he obtained for a 12-day period of fair weather and weak synoptic-scale forcing during PASTEX (23 July until 3 August 1994). The katabatic flow exhibits a semi-diurnal cycle, with largest vertical extent (and wind speeds) late at night and in the late afternoon. Van den Broeke suggests that the late night maximum is associated with mass flux towards the glacier from the cooling valley walls, not to radiative cooling at the surface (note that the surface is at the melting point all the time). The maximum in the late afternoon is due to the maximum in buoyancy forcing, because at this time the air filling the valley reaches its maximum temperature. The development and decay of the valley wind are clearly seen. Typical wind speeds are 2 m/s and a characteristic temperature range across the day is 5 K.

To conclude this section, Figure 6 presents some statistics on the relation between the height and magnitude of the wind maximum from PASTEX. Denby (1996) analysed data for a two-week period in which glacier wind occurred during 95 % of the time. Maximum wind speed (u_m) and height of the wind maximum (z_m) were determined by polynomial fitting to the 30-min mean data values. There is a correlation between maximum wind speed and temperature at 13 m, but it is not strong. The same applies to other combinations of parameters. For instance, there is a 0.4 correlation between 2 m wind speed and 13 m temperature, but no significant correlation between 2 m wind speed and 2 m temperature. The temperature observations at larger

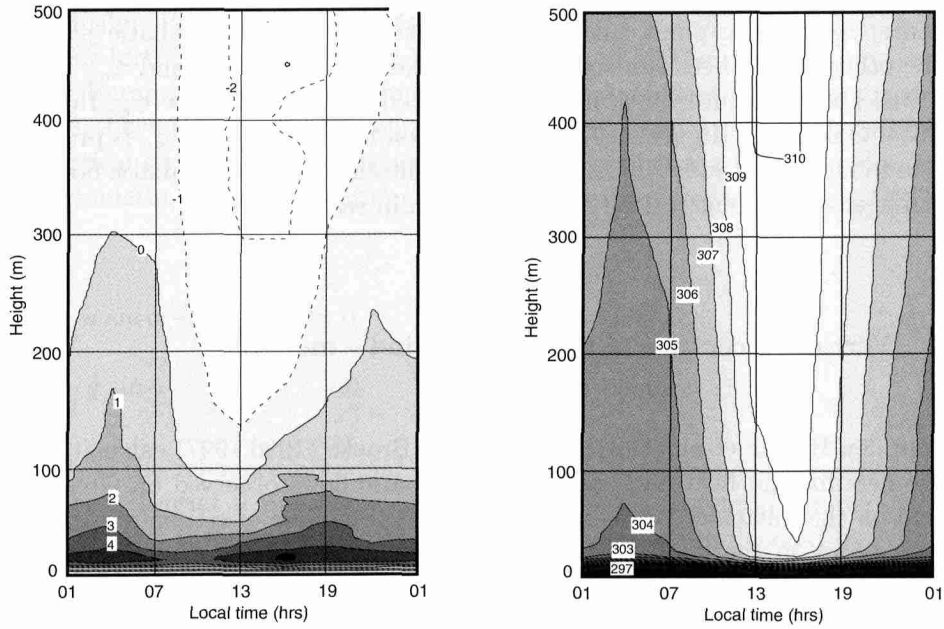

Fig. 5. Daily cycle of downslope wind speed and potential temperature as measured with balloon soundings during PASTEX. The patterns shown are the mean for a 12-day period in summer with weak synoptic-scale forcing (from Van den Broeke, 1996).

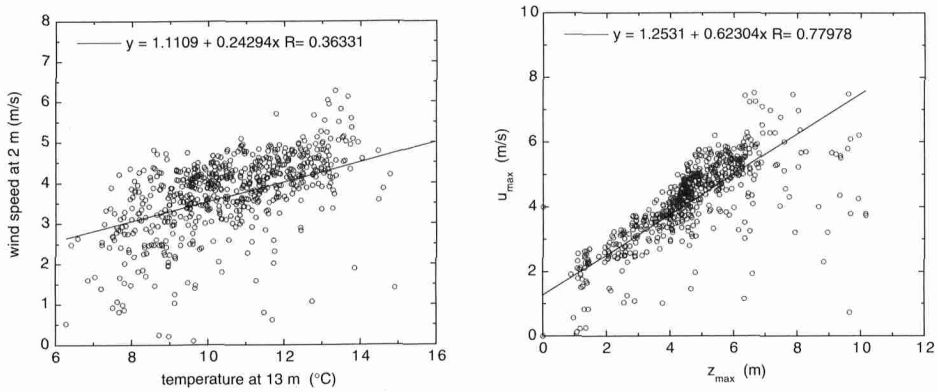

Fig. 6. Scatter plot of 2 m wind versus 13 m temperature (left) and maximum wind speed versus height of wind maximum, as measured during PASTEX with a profile mast. Each data point represents a 30 min average. Provided by B. Denby, based on data supplied by P. Smeets.

heights are very probable a better measure of the katabatic forcing (which, in this case, is basically determined by the difference between surface temperature, i.e. melting point, and the temperature above the katabatic jet). On the other hand, there is a significant correlation between u_m and z_m. This is a well-known feature which has been reported in earlier studies (e.g. Hoinkes, 1954; Ohata and Higuchi, 1979). The relation between u_m and z_m is probably due to increasing eddy diffusivity for momentum when the katabatic flow gets stronger. This point will be discussed again in section 8.

5 Vertical structure of the glacier wind - modelling

Van den Broeke et al. (1994) and Van den Broeke (1996,1997) calculated the momentum and heat budgets for the katabatic flows observed on Greenland and on the Pasterze. We will not discuss his technique of estimating the various terms in the budget equations, but merely mention a few results. For down-slope momentum the leading terms are buoyancy forcing and friction. This applies both to the Greenland ice sheet and the Pasterze. The Coriolis force is less important (less than 20% of the buoyancy forcing). For cross-slope momentum on the Greenland ice sheet there is a good balance between Coriolis force and friction. Note, however, that the cross-slope flow is significantly weaker than the downslope flow, as mentioned earlier (see also Figure 1).

The leading terms in the heat budget are the sensible heat flux and vertical advection in the stably stratified atmosphere. Divergence of the radiative flux plays a minor role. In both the heat and momentum budgets horizontal advection does not appear as a significant term. As was already suggested by Kuhn (1978), this implies that the structure of the katabatic flow over melting ice is not determined by the horizontal length scale, but by local parameters like surface roughness, slope, and static stability of the atmosphere. It remains unclear how general such a conclusion is. In spite of the fact that the data sets used are currently the best available for this purpose, they are still not really adequate to resolve the three-dimensional structure of the katabatic flow and its variation in time. Most theoretical models for katabatic flows have followed a hydraulic approach, in which vertically-integrated momentum and heat equations are used e.g. (Manins and Sawford, 1979; Ohata, 1989). Nevertheless, the vertical structure of the glacier wind appears so typical and well defined that it is the first thing to be explained. Results from numerical models concerning the dynamics of katabatic flows have been reported in a number of publications e.g. (Yamada, 1981; McNider and Pielke, 1984; Parish, 1984; Meesters et al., 1994). It should be noted, however, that only in a few cases a detailed comparison of the vertical structure in numerical results and measurements has been attempted (Denby, 1996).

The interpretation of the recently obtained data, as described at the

beginning of this section, lends support to the original ideas of Prandtl (1942) on slope winds. Although this model has been discussed, accepted (e.g. Lettau, 1966; Kuhn, 1978) and rejected (e.g. Martin, 1975), it will be used here as a basis for further theoretical considerations. First of all the theory is repeated briefly. Retaining the leading terms in the heat and momentum budgets as described above leads to a relatively simple set of dynamic equations describing the vertical structure of the glacier wind. These read (for a full discussion on the formulation of the momentum balance for gravity flows, see Mahrt, 1982):

$$\gamma\, u \sin\alpha + \frac{d}{dz}\overline{(w'\theta')} = 0 \qquad \text{(heat balance)}\ , \tag{1}$$

$$\frac{\theta}{\theta_0}\, g \sin\alpha + \frac{d}{dz}\overline{(w'u')} = 0 \qquad \text{(momentum balance)}\ . \tag{2}$$

Here θ_0 is the reference potential temperature, g acceleration of gravity, γ a constant potential temperature lapse rate and θ the potential temperature deficit [2]. The turbulent fluxes of heat and momentum are denoted by $\overline{(w'\theta)}$ and $\overline{(w'u')}$. The surface is tilted by an angle α with respect to the horizontal. The velocity parallel to the ice surface is denoted by u (note that the z-axis is not vertical, but perpendicular to the glacier surface). So θ and u are the dependent variables.

Equations (1) and (2) can be considered as the simplest set describing the dynamics of the glacier wind. To find a first basic solution to these equations we consider the case where the fluxes of heat and momentum are formulated with simple K-theory:

$$\overline{w'\theta'} = -K_h \frac{d\theta}{dz} \quad ; \quad \overline{w'u'} = -K_m \frac{du}{dz}\ . \tag{3}$$

Here K_m and K_h are the eddy diffusivities for momentum and heat, assumed to be constant with z. The model then reduces to the classical Prandtl model for slope winds (Prandtl, 1942; discussed in more detail and including a comparison with some field data by Defant, 1949). We note immediately that the Prandtl-model cannot be valid close to the surface because the eddy diffusivities do not go to zero. In contrast, the strength of this model lies in the fact that it retains the coupling of the thermal and motion fields, and it allows to obtain an analytic solution. Equations (1)–(3) are easily combined into a 4th-order equation for the temperature perturbation:

$$\frac{d^4\,\theta}{dz^4} - \frac{\gamma\, g \sin^2\alpha}{T_0\, K_m\, K_h}\,\theta = 0\ . \tag{4}$$

[2] The actual potential temperature minus the background temperature.

For θ_0 we now use the melting point, denoted by T_0. The boundary conditions can be are formulated as:

$$z = 0 \qquad u = 0 \quad \text{and} \quad \theta = C \ , \tag{5}$$
$$z \to \infty \qquad u = 0 \quad \text{and} \quad \theta = 0 \ . \tag{6}$$

Here C is the "temperature deficit" at the surface ($C < 0$). It is easily verified that the solution fulfilling these conditions reads:

$$\theta = C\, e^{-z/\lambda}\, cos(z/\lambda) \ , \tag{7}$$
$$u = -C\, \mu\, e^{-z/\lambda}\, sin(z/\lambda) \ , \tag{8}$$

$$\text{where} \quad \lambda = \sqrt[4]{\frac{4\, T_0\, K_m\, K_h}{\gamma\, g\, \sin^2 \alpha}} \quad \text{and} \quad \mu = \sqrt{\frac{g\, K_h}{T_0\, \gamma\, K_m}} \ . \tag{9}$$

Here λ appears as the natural length scale of the flow. It increases with eddy diffusivity ($O^{1/2}$) and decreases with potential temperature lapse rate ($O^{-1/4}$) and surface slope $O^{-1/2}$.

From eq. (8) it is found that the height at which the wind maximum occurs reads

$$z_m = \frac{\pi}{4}\, \lambda \ . \tag{10}$$

It is also easily verified that the maximum wind speed is

$$u_m = -C\, \mu\, e^{-\pi/4}\, sin(\pi/4) = -a_1\, C\, \mu \ . \qquad (a_1 = 0.322) \tag{11}$$

It should be noted that the maximum wind speed depends on the strength of the temperature forcing (C) and on K_h/K_m (later denoted by β), but not on the absolute values of the eddy diffusivities. To plot the solution in non-dimensional form, temperature can be scaled with C and wind speed with $C\mu$. The result is shown in Figure 7a. It can be seen that the basic structure of the glacier wind is present in the solution, which, given the simplicity of the model, is a nice result.

The fluxes of momentum and heat, F_m and F_h respectively, are

$$F_m = \frac{\mu\, C\, K_m}{\lambda}\, e^{-z/\lambda}\, (cos(z\lambda) - sin(z\lambda)) \ , \tag{12}$$
$$F_h = \frac{C\, K_h}{\lambda}\, e^{-z/\lambda}\, (cos(z\lambda) + sin(z\lambda)) \ . \tag{13}$$

The non-dimensional flux profiles are shown in Figure 7b. The momentum flux, of course, changes sign at the wind maximum. It should be noted that

the momentum and heat fluxes, irrespective of the sign, have different shapes. The momentum flux increases more and more when approaching the surface, whereas the heat flux tends to a constant value.

Obviously, the Prandtl-model should be critisiced on two points. First of all, since eddy diffusivity does not decrease when the surface is approached, the steep velocity gradient close to the surface, normally formulated in the log or log-linear wind profile for a constant-flux layer, is not reproduced. Secondly, in the Prandtl-model the katabatic jet is more pronounced than it is in reality. Although the appearance of a wind maximum at low height is a stable feature in the data, the observed decrease in wind velocity when going upward is much slower than in the model. This is in contrast to what one would expect. By using a constant eddy diffusivity it would be more logical to see a model jet that is too diffuse rather than too sharp. At this point it is interesting to compare the Prandtl solution with the outcome of more sophisticated modelling.

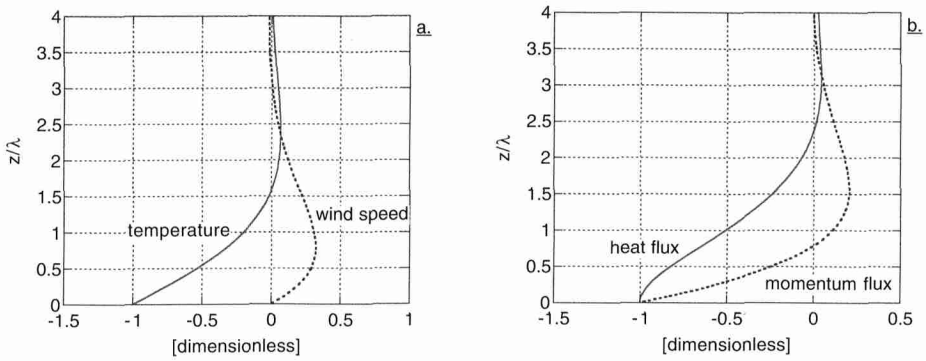

Fig. 7. Temperature and wind profiles calculated with the Prandtl-model (a). The associated fluxes of momentum and heat are also shown (b).

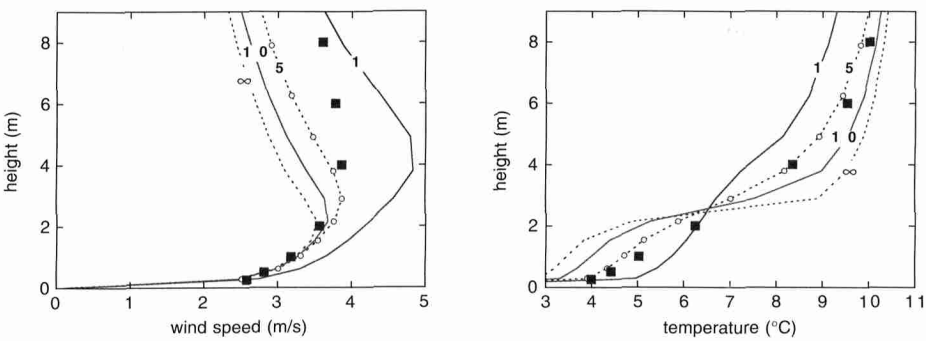

Fig. 8. Temperature and wind profile as simulated with a 2-d dynamic model with a 1.5 closure scheme for turbulent exchange. Profiles are shown for various values of ϕ_{max} (see text), as labelled on the curves. Black squares show observations. Vertical grid-resolution of the model is seen on the curve for $\phi_{max} = 5$. From Denby (1996).

Denby (1996) made a detailed numerical model study of the glacier wind over the Pasterze. His model is two-dimensional (vertical plane along valley axis), has variable grid spacing to resolve the glacier wind well, and used a terrain-following vertical coordinate and surface-orthogonal grid for optimal representation of the meteorological fields close to the glacier surface. Turbulent diffusion is modelled with 1.5-order closure with local scaling. One of the difficulties in such an approach is that too little mixing occurs near the wind maximum. In many studies on katabatic jets this problem is "solved" by imposing a maximum value ϕ_{max} on the nondimensional velocity gradient. Denby (1996) has run his model for many sets of parameters during longer periods of time (days). It yields a simulation of the glacier-valley wind and its daily cycle which is quite reasonable. When looking at details, however, some notable differences between the calculations and the observations are evident. For a full discussion the reader is referred to Denby (1996). Here we look at the dependence of the simulated glacier-wind and temperature profiles on ϕ_{max} (Figure 8). The figure shows that the choice of ϕ_{max} determines the shape of the profiles to a large extent. A value of about 5 appears best. However, the model has difficulty in simulating the observed velocity gradient above the wind maximum. In this respect it has the same deficiency as the simple Prandtl-model.

6 Surface fluxes

From the point of view of glacier mass balance modelling, the fluxes of heat and moisture at the surface are the most interesting. Although the theory for fluxes in the horizontal homogeneous boundary layer appears well developed (see e.g. Nieuwstadt and Duynkerke, 1996), applying it to the flow over melting glaciers is problematical. It is difficult to define the relevant length scales. The top of the boundary layer is hard to identify. Another serious problem is that the depth of the surface layer is unclear. Since the forcing of the flow is largest near the surface, where the temperature deficit reaches its maximum value, a constant flux layer will be very shallow. Once the snow has disappeared from the surface and the ice begins to melt unevenly, the characteristic obstacle height quickly reaches values of typically 1 m (Figure 9). With a wind maximum at a height generally between 3 and 10 m, this implies that a surface layer cannot be much thicker than the characteristics obstacle height. Consequently, part of the flow will be along ice bumps rather than across them.

The implication of this complicated geometric structure is twofold. Firstly, there is the question of how to measure representative profiles of wind, temperature and humidity. Secondly, even if representative profiles are obtained, it is unclear whether a bulk method or integrated flux-profile relationships can be used to estimate the surface fluxes, because the existence of

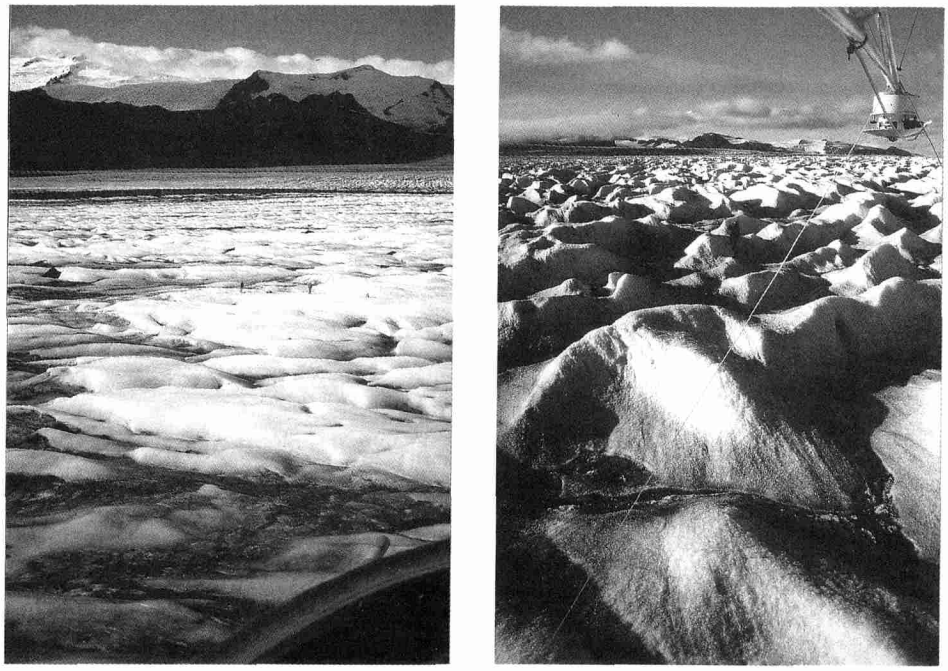

Fig. 9. Photographs taken on Vatnajökull (Iceland) in the summer of 1996, showing the irregularity of a melting glacier surface. The left picture, taken from a helicopter, shows the lower ablation zone. Two persons are standing in the middle. Note the large variation in topography and albedo. The right picture was taken higher up in the ablation zone, where the characteristic obstacle size is about 2 m. A person can be seen just above the middle of the picture. Photos by P. Smeets.

a constant flux layer of sufficient depth cannot be demonstrated. There are two ways of estimating fluxes to test a bulk or profile method. One way is to perform eddy correlation measurements. This has been done on melting glaciers in a few field campaigns, as will be discussed shortly. The other way is to solve the turbulent heat flux by closing the surface energy budget (residual method). This can be done when radiation balance, subsurface heat flux and mass exchange rates are measured accurately. In practice sufficient accuracy cannot be obtained, unless a period is selected in which the glacier surface is melting all the time (temperature and vapour pressure at the surface are than known accurately).

The residual method has been applied by several authors, including Kuhn (1979), Hay and Fitzharris (1988) and Van den Broeke (1996, chapter 5). Munro (1989) was one of the first to make a comparison between bulk estimates of the heat flux and eddy correlation measurements on a melting glacier tongue. He collected data on Peyto Glacier, Rocky Mountains, Canada. Munro clearly identifies the zero-referencing problem, and his Figure 2, shown here as Figure 10, provides a striking illustration. Calculating mean roughness lengths for momentum (z_0) and heat (z_T) from profile analysis, he found that

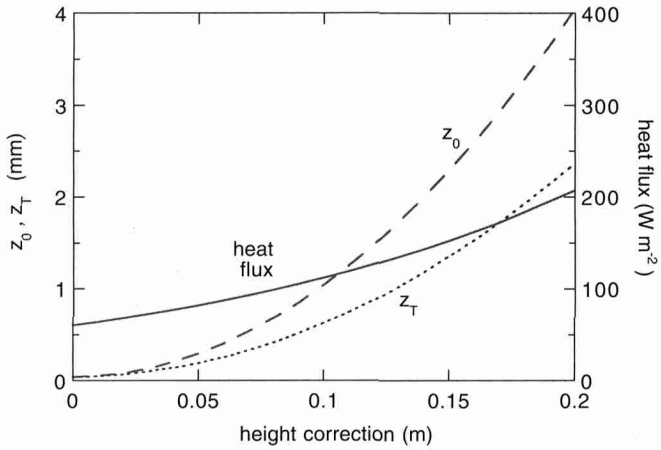

Fig. 10. The effect of height correction on the calculation of roughness length and surface fluxes from profile analysis, illustrating the zero-reference problem. Redrawn from Munro's (1989) study on Peyto Glacier, Canada.

the result was very sensitive to the choice of zero-reference level. The figure shows the dependence of z_0, z_T and associated sensible heat flux on a height correction. The conclusion must be that on a melting glacier surface it is very difficult to obtain accurate estimates of the sensible heat flux by the profile method.

Another conclusion reached by Munro (1989) was that good agreement between eddy correlation measurements and the bulk method could be obtained if z_0 is estimated from microtopographic data rather than from profile analysis, following Lettau's (1969) expression:

$$z_0 = 0.5\, h^* \frac{s}{S} \,. \tag{14}$$

Here h^* is the effective height of roughness elements, s is the silhouette area of roughness elements measured perpendicular to the wind direction, and S is the number of elements per unit area. Van den Broeke (1996), in his analysis of the energy budget data from GIMEX, came to the same conclusion. Using values of z_0 from profile analysis, he was unable to explain the turbulent heat flux as found by closure of the energy balance (residual method). Estimating z_0 by the microtopographic method, either following Lettau (1969) or Banke et al. (1980), gave a value of z_0 which was two orders of magnitude larger. In order to calculate the heat flux, he used (as did Munro, 1989) Andreas' (1987) expression for the relation between z_0 and z_T :

$$ln(\frac{z_T}{z_0}) = 0.317 - 0.556\, ln(Re) - 0.183\, ln^2(Re) \,. \tag{15}$$

Here Re is the roughness Reynolds number defined as

$$Re = \frac{u^* z_0}{\nu} , \tag{16}$$

where u^* is the friction velocity and ν the kinematic viscosity. The outcome showed good agreement between the calculated turbulent heat flux and the flux obtained by the residual method, thus confirming the conclusion of Munro about the usefulness of a topographic method to determine z_0 .

7 Deriving Fluxes with a modified Prandtl model

Given the problems in applying established theory and methods to derive fluxes in the glacier wind, an alternative approach is to use a modified form of the Prandtl-model. Since the katabatic jet is driven totally by the heat exchange between surface and overlying air, the best information on the magnitude of this exchange must be contained in the bulk properties of the jet. In this jet the temperature and momentum fields are fully coupled. In an approach in which this coupling is ignored, as in the standard profile analysis, information is lost. In fact, fitting of the Prandtl solution to observations for estimating the surface heat flux was proposed and illustrated by Kuhn (1978). He shows that, under certain assumptions, the heat flux can be estimated from the height of the wind maximum in combination with the surface slope, potential temperature lapse rate and temperature forcing (-C in the current notation). In the forthcoming analysis basically the same idea will be used and extended.

As noted earlier, the Prandtl model cannot be correct close to the glacier surface. Therefore matching with a surface-layer model is desirable. Unfortunately, observations do not give enough detail on the structure and depth of the surface layer to provide guidance. It is doubtful whether a straightforward matching with log-linear profiles for wind speed and temperature makes sense. From the nature of the katabatic flow it appears that the surface layer will be shallow, with a depth of at most $\lambda/5$ m. In many cases, as argued earlier, this is not much deeper that the characteristic obstacle size on a melting glacier surface and it remains impossible to define the zero-height reference. Nevertheless, it is a fact that close to the surface the gradients predicted by the Prandtl-model are far too small.

As a pragmatic approach, one could simply restrict the validity of the Prandtl-model to heights above a certain fraction of the katabatic length scale λ. In effect this implies a downward shift of the theoretical temperature and wind profiles, as illustrated in Figure 11. The fluxes at the top of the surface layer can be evaluated from

$$F_m = \frac{\mu C K_m}{\lambda} e^{-(1-\nu)} \left(cos(1-\nu) - sin(1-\nu)\right) , \tag{17}$$

$$F_h = \frac{C K_h}{\lambda} e^{-(1-\nu)} \left(cos(1-\nu) + sin(1-\nu)\right) . \tag{18}$$

If the surface layer is considered to be a constant flux layer, these expressions then also provide an estimate of the surface fluxes. To illustrate the idea, the model described in the section 5 has been fitted to the wind and temperature profiles as shown in the first panel of Figure 4 (day 210, 00 UT). This yields the result displayed in Figure 12a. Parameter values taken are: C = -10 K, γ = 0.004 K m^{-1}, K_m = 0.9 m^{2}s^{-1}, β = 0.3, ν = 0.75. The corresponding value for the katabatic length scale is λ = 9.8 m.

It should be noted that the parameter values are well defined. As can be seen from eq. (9)–(11), the value of β affects only the maximum wind speed, not the height at which the maximum occurs. If eddy diffusivity for momentum and heat were to be equal (β=1), an unrealistically large value for the temperature stratification (γ) would be needed to obtain the correct wind speed. The momentum flux at the top of the surface layer is -0.066 m^{2}s^{-2}, the sensible heat flux 0.025 K m s^{-1}. To obtain the surface heat flux in W m^{-2}, F_h should be multiplied by ρc_p (about 1000 J m^{-3}K^{-1} for the altitude considered). It is obvious from Figure 12a that the optimal value for ν is different for the velocity and the temperature profile. Figure 12b shows the fits when ν is taken to be different for momentum and temperature. Apparently, the surface layer for temperature seems to be deeper than for momentum. It should be noted, however, that choosing different values for ν introduces a (minor ?) inconsistency into the dynamic formulation for the katabatic flow. Fortunately, with regard to the calculated heat flux it makes little difference what procedure is taken.

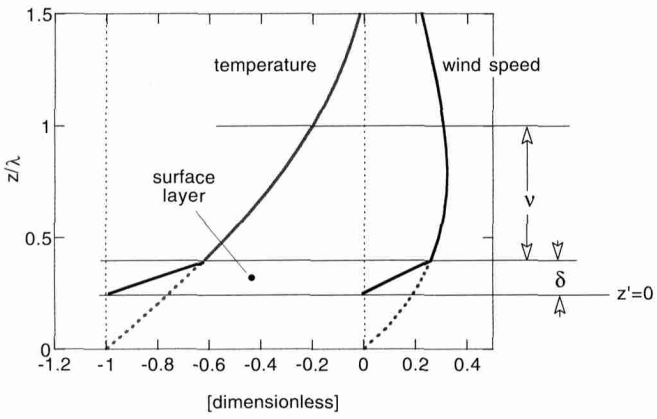

Fig. 11. As figure 7a, but here the lower part of the Prandtl solution is replaced by a shallower surface layer of nondimensional depth δ.

8 The Prandtl model with flow-dependent eddy diffusivity

In the previous section the Prandtl model was fitted to an observed profile by choosing suitable values for some model parameters, including the eddy diffusivities. It seems unlikely that the eddy diffusivities will be the same for stronger or weaker flow. One might think that the relation between u_m and z_m, as for instance seen in Figure 6b, is due partly to the dependence of turbulent mixing on the strength of the katabatic flow. In this respect it should be noted that z_m does not depend on C, so in the original Prandtl model the height of the wind maximum does not vary with C.

It is possible to introduce variable mixing capacity in the Prandtl model by assuming that the relevant scales for eddy mixing are proportional to u_m and λ. One of the arguments for this is the presence of relatively large eddies and (breaking ?) waves in the glacier wind, probably induced by interaction of the katabatic jet with the marked 3-dimensional topography (see Figure 9). So we have

$$K_m = k\,\lambda\,u_m = -a_1\,k\,\lambda\,\mu\,C\ . \tag{19}$$

With the parameter β included, the original expressions for u_m and λ read:

$$u_m = -a_1\,C\,\mu = -a_1\,C\sqrt{\frac{g\,\beta}{T_0\,\gamma}}\ , \tag{20}$$

$$\lambda = \sqrt[4]{\frac{4\,T_0\,\beta\,K_m^2}{g\,\gamma\,\sin^2\alpha}}\ . \tag{21}$$

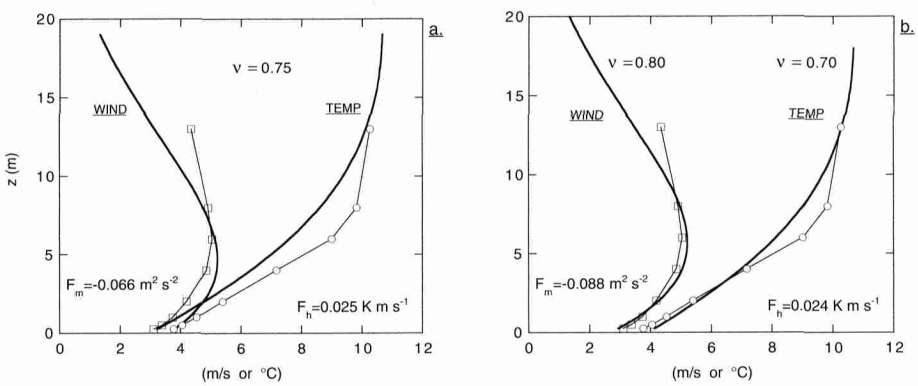

Fig. 12. Fitting the Prandtl-model to the observed temperature and wind profiles during PASTEX at 00 UT, 29 July 1994 (first panel in Figure 4). In (a) profiles are shifted over a nondimensional distance (1-ν)=0.25. In (b) the shift has been done independently for temperature and wind speed.

Substitution of eq. (19) in eq. (21) yields

$$\lambda = \pm\sqrt{\frac{4\,T_0\,\beta\,k^2\,a_1^2\,\mu^2\,C^2}{g\,\gamma\,\sin^2\alpha}} = -\frac{2\,a_1\,k\,\beta\,C}{\gamma\,\sin\alpha}\ . \tag{22}$$

The solution with the + sign is dropped because it would give a negative value of λ (remember that $C < 0$). So a simple expression for the katabatic length scale is found: it is proportional to the temperature forcing $|C|$ divided by the background lapse rate projected along the glacier surface.

Whereas the dimensionless solution remains the same of course, the dependence of the coefficients on the forcing is different now. This is illustrated in Figure 13. Here parameters, given in the caption, have been chosen such that the results are in broad agreement with what is observed on glaciers, but no detailed fitting has been done. It should be noted that at this stage a value for δ, the nondimensional depth of the surface layer, has to be chosen to relate z (height in the Prandtl formulation) to the real height z', i.e. (see Figure 11):

$$z' = z - \lambda(1 - \nu - \delta)\ . \tag{23}$$

The value for δ used here (0.1) implies that the depth of the surface layer is typically 10% of the height at which the wind maximum occurs. In Figure 13 results are plotted as a function of $-C$, i.e. the temperature difference between the air above the katabatic regime and the surface. First of all, a realistic relation between the height and strength of the wind maximum is

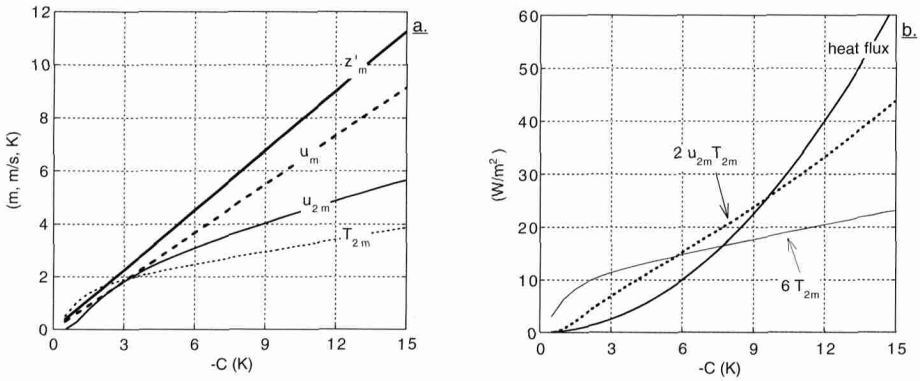

Fig. 13. Results from the modified Prandtl-model. (a) Dependence of height of wind maximum (z'_m), maximum wind speed (u_m), wind speed at 2 m (u_{2m}) and temperature at 2 m (T_{2m}) on the thermal forcing C. The heat flux is shown in (b), together with two curves illustrating parameterizations of the heat flux that have been used in glacier mass-balance models. Parameter values: $\delta = 0.1$, $\nu = 0.75$, $\beta = 0.3$, k = 0.16, $\gamma = 0.004$ K/m, $\alpha = 5°$.

now evident. The ratio u_m/z'_m is in broad agreement with the slope of the linear regression in Figure 6b. According to the present model, this slope is given by

$$\frac{u_m}{z'_m} = \frac{\sin\alpha}{2\,k\,(\pi/4 - 1 + \nu + \delta)}\sqrt{\frac{g\,\gamma}{\beta\,T_0}}\,. \tag{24}$$

Wind speed and temperature at 2 m height are also plotted in Figure 13a, since these are frequently measured quantities. The relation between C and the 2 m temperature and wind speed is nonlinear for smaller values of $|C|$. For larger values of $|C|$ the increase in the 2 m temperature is linear but small, in accordance with what is observed in the field.

In Figure 13b the heat flux (defined now as $-\rho c_p F_h$, where ρc_p has been set to 1000 J m^{-3}K^{-1} to give it a characteristic value) is shown. The heat flux increases nonlinearly with the forcing $|C|$. For comparison, two additional curves are shown reflecting bulk parameterisations of the heat flux that have been used in glacier mass-balance models. These are $c_1 T_{2m}$ and $c_2 u_{2m} T_{2m}$. Irrespective of the choice of c_1 and c_2 (in the figure 6 W m^{-2}K^{-1} and 2 W s m^{-3} K^{-1}), a good fit cannot be obtained. So one has to conclude that the modified Prandtl model does not support the use of simple bulk formulations to calculate the heat flux from measurements of temperature and wind speed at a height of 2 m.

Next we discuss the possibility of a stability correction in the formulation for the eddy diffusivity. For the katabatic flow considered here a bulk Richardson number may be defined as:

$$R_b = \frac{-g\,C\,\lambda}{T_0\,u_m^2}\,. \tag{25}$$

Substituting the expressions for λ and u_m leads to:

$$R_b = \frac{2k}{a_1\,\sin\alpha}\,. \tag{26}$$

So it appears that R_b becomes independent of the forcing C and the stratification γ. This is a remarkable result, implying that a stability correction in the formulation for the eddy diffusivities is not feasible. It should be noted, however, that K_m still depends significantly on γ. Since both λ and μ decrease with increasing γ, eddy mixing decreases with increasing stratification.

In spite of its simplicity, it appears that the modified Prandtl model proposed here is capable of explaining many of the observed features associated with glacier wind. Mixing-length theory has been applied in a crude way. The present theory combines the vertical resolution of the Prandtl model with a bulk approach for the determination of the eddy diffusivity. Also, the dynamic

coupling of temperature and motion field is retained. The katabatic jet ows its existence to the surface heat flux. It is thus natural to assume that this heat flux can be estimated from the characteristics of the jet. Nevertheless, a more thorough comparison with observations is needed before the value of this approach can be fully judged.

Epilogue

The following conclusions emerge from this chapter:

- Over melting glacier surfaces, katabatic flow is present most of the time, even when there is strong exposure to synoptic-scale weather systems. The katabatic flow shapes the microclimate of a glacier in summer.
- It is difficult to apply existing theory for the stable boundary-layer to the glacier wind. Because of the large obstacle size compared to the height of the wind maximum in combination with the stable stratification, there is a serious zero-referencing problem. It is questionable whether a surface layer can be identified in the usual way.
- For the calculation of surface fluxes with bulk methods it is best to determine the roughness length z_0 with a microtopographic method. The zero-referencing problem mentioned implies that profile analysis leads to poorly defined values of z_0.
- To retain the coupling between heat and momentum field, it is proposed that a modified Prandtl-model be used to estimate surface fluxes and to study the sensitivity of these fluxes to changes in the large-scale variables.

It is obvious that the modified Prandtl-model for estimating the surface heat flux should be tested extensively. This can be done partly with existing data, but also more eddy correlation measurements need to be carried out. In such experiments much attention should be given to spatial variability. Inevitably, this implies the simultaneous use of a number of eddy correlation instruments mounted at one nominal height on a transect across a bumpy ice surface.

Acknowledgements

Most of this chapter is based on the glacio-meteorological experiments listed in Table I. These experiments were carried out with a relatively small group of highly motivated and skilled people. In those experiments the Institute for Marine and Atmospheric Research (Utrecht University) took the lead, but everything would have been far more difficult without the intense cooperation of three other research institutions: the Science Institute of the University of

Iceland (Prof. Helgi Björnsson), the Faculty of Earth Sciences of the Vrije Universiteit Amsterdam (Prof. H.F. Vugts), and the Institute for Meteorology and Geophysics of the University of Innsbruck (Prof. M. Kuhn). Support for the glacio-meteorological experiments came from the Netherlands Research Programme on Global Air Pollution and Climate Change (NOP 850016), the Netherlands Organization for Scientific Research (through the Netherlands Geosciences Foundation), the European Commission (EPOC CT90-0015, EV5V-CT91-0051, ENV4-CT95 -0105), the National Power Company of Iceland, the University of Iceland Research Fund and the Iceland Glaciological Society.